^{3}He impurity excitation spectrum in liquid ^{4}He

A. Fabrocini
Istituto Nazionale di Fisica Nucleare, Dipartimento di Fisica, Università di Pisa, I-56100 Pisa, Italy

A. Polls
Departament d'Estructura i Constituents de la Matèria, Universitat de Barcelona, E-08028 Barcelona, Spain
(Received 25 March 1998)

We microscopically evaluate the excitation spectrum of the ^{3}He impurity in liquid ^{4}He at $T=0$ and compare it with the experimental curve at equilibrium density. The adopted correlated basis perturbative scheme includes up to two independent phonons, intermediate correlated states, and the correlation operator is built up with two- and three-body correlation functions. The experimental spectrum is well described by the theory along all the available momentum range. A marked deviation from the simple Landau-Pomeranchuck quadratic behavior is found and the momentum-dependent effective mass of the impurity increases by $\sim 50\%$ at $q \sim 1.7$ Å^{-1} with respect to its $q=0$ value. No signature of rotonlike structures is found.
[S0163-1829(98)05233-3]

Both experimentalists and theoreticians have devoted a great deal of effort to measure and explain the characteristics of one ^{3}He impurity in atomic liquid ^{4}He. From the experimental point of view it is well known how the impurity chemical potential μ_3 behaves with temperature and pressure,[1] its effective mass m_3^* and quasiparticle excitation spectrum $e(q)$.[2,3] In Ref. 3 the authors found a sizable deviation from the quadratic Landau-Pomeranchuk (LP) spectrum,[4] $e_{\rm LP}(q)=\hbar^2 q^2/2m_3^*$, in low concentration ^{3}He-^{4}He mixtures. $e(q)$ was parametrized in a modified LP (MLP) form as

$$e_{\rm MLP}(q)=\frac{\hbar^2 q^2}{2m_3^*}\frac{1}{1+\gamma q^2}. \tag{1}$$

The estimated values of the MLP parameters, at $P=1.6$ bar and $x_3\sim 0.05$ ($x_3=^3$He concentration) are $m_3^*\sim 2.3 m_3$ and $\gamma\sim 0.13$ Å^2.

Microscopic calculations, done in the framework of the correlated basis function (CBF) perturbation theory,[5] have been able to give good estimates of μ_3 and m_3^* at the $T=0$ ^{4}He equilibrium density $\rho_{\rm eq}=0.02185$ Å^{-3}. Recently, a diffusion Monte Carlo approach has provided similar results.[6] There are also theoretical indications of a deviation of the spectrum from the LP form.[7,8] The presence of a possible rotonlike structure in $e(q)$ near the crossing with the ^{4}He phonon-roton spectrum was supposed in Ref. 9 but not confirmed in Refs. 7, 8. However, in Ref. 8 an excitation spectrum quite higher than the experimental one was found.

Here we will employ the CBF machinery of Ref. 5 (hereafter denoted as I) to compute, in a microscopic way, the whole impurity spectrum. The CBF basis used in I consisted in correlated n-phonon states

$$\Psi_{\mathbf{q};\mathbf{q}_1\cdots\mathbf{q}_n}=\rho_3(\mathbf{q}-\mathbf{q}_1-\cdots-\mathbf{q}_n)\rho_4(\mathbf{q}_1)\cdots\rho_4(\mathbf{q}_n)\Psi_0, \tag{2}$$

where $\rho_4(\mathbf{k})=\Sigma_{i=1,N_4}e^{i\mathbf{k}\cdot\mathbf{r}_i}$ is the ^{4}He density fluctuation operator and $\rho_3(\mathbf{k})=e^{i\mathbf{k}\cdot\mathbf{r}_3}$ describes the excitation of the impurity. The basis states were then properly normalized. $\Psi_0=\Psi_0(3,N_4)$ is the ground state wave function of N_4 ^{4}He atoms plus one ^{3}He impurity of volume Ω, taken in the N_4, $\Omega\to\infty$ limit, at constant ^{4}He density $\rho_4=N_4/\Omega$.

A realistic choice for $\Psi_0(3,N_4)$ is made by applying an extended Jastrow-Feenberg correlation operator[10] to the noninteracting g.s. wave function

$$\Psi_0(3,N_4)=F_2(3,N_4)F_3(3,N_4)\Phi_0(3,N_4). \tag{3}$$

$F_{2,3}$ are N-body correlation operators including explicit two- and three-body dynamical correlations. F_2 is written as a product of two-body Jastrow, ^{3}He-^{4}He and ^{4}He-^{4}He correlation functions

$$F_2(3,N_4)=\prod_{i=1,N_4} f^{(3,4)}(r_{3i})\prod_{m>l=1,N_4} f^{(4,4)}(r_{lm}), \tag{4}$$

and F_3 is given by the correspondent product of triplet correlations $f^{(\alpha,\beta,\gamma)}(\mathbf{r}_\alpha,\mathbf{r}_\beta,\mathbf{r}_\gamma)$.

The correlation functions are variationally obtained by minimizing the g.s. energy of the system E_0. The procedure is outlined in I, where a parametrized form for the triplet correlations was used and the Jastrow factors were obtained by the Euler equations $\delta E_0/\delta f^{(\alpha\beta)}=0$. The equations were solved within the hypernetted chain (HNC) framework and the *scaling* approximation for the elementary diagrams.[11] The Aziz interatomic potential[12] was used in the minimization process.

The perturbative calculation of I included one independent phonon (OIP) and two independent phonon (TIP) states and all the diagrams corresponding to successive rescatterings of the one phonon (ROP) states. This contribution was obtained by solving a Dysonlike equation in the correlated basis. While the correlation factors are intended to care for the short-range modifications of the ground state wave function due to the strongly repulsive interatomic potential, the

basic physical effect induced by the perturbative corrections may be traced back to the backflow around both the impurity and the ^{4}He atoms. The CBF analysis provided $\mu_3(\mathrm{CBF}) = -2.62$ K [vs $\mu_3(\mathrm{expt}) = -2.79$ K] and $m_3^*(\mathrm{CBF}) = 2.2 m_3$ at equilibrium density. The chemical potential was obtained with the Lennard-Jones potential and some improvement may be expected by the Aziz interaction.

In order to construct the CBF perturbative series, we write $e(q) = e_0(q) + \Delta e(q)$, with $e_0(q) = \hbar q^2/2m_3$ and

$$\Delta e(q) \sim \Delta e_{\mathrm{OIP}}(q) + \Delta e_{\mathrm{TIP}}(q) + \Delta e_{\mathrm{ROP}}(q). \tag{5}$$

The different terms in Eq. (5) represent contributions from the corresponding intermediate states. The n-phonon states have been Schmidt-orthogonalized to states with a lower number of phonons. For instance, the actual OIP state reads

$$|\mathbf{q};\mathbf{q}_1\rangle = \frac{|\Psi_{\mathbf{q};\mathbf{q}_1}\rangle - |\Psi_{\mathbf{q}}\rangle\langle\Psi_{\mathbf{q}}|\Psi_{\mathbf{q};\mathbf{q}_1}\rangle}{\langle\Psi_{\mathbf{q};\mathbf{q}_1}|\Psi_{\mathbf{q};\mathbf{q}_1}\rangle^{1/2}}. \tag{6}$$

The two-phonon state $\Psi_{\mathbf{q};\mathbf{q}_1\mathbf{q}_2}$ has been orthogonalized in a similar way to $\Psi_{\mathbf{q}}$, $\Psi_{\mathbf{q};\mathbf{q}_1+\mathbf{q}_2}$, and $\Psi_{\mathbf{q};\mathbf{q}_{1,2}}$. The orthogonalization is a necessary step in fastening the convergence of the series as the nonorthogonalized states have large mutual overlaps.

The nondiagonal matrix elements (ME's) of the Hamiltonian H (we remind the reader that we use the Aziz potential) are evaluated by assuming that the two- and three-body correlations are solutions of the corresponding Euler equations. This is not strictly true for the triplet correlations but the corrections are expected to be small. With this assumption, it is easily verified that

$$\langle\mathbf{q}|H|\mathbf{q};\mathbf{q}_1\rangle = -[N_4 S(q_1)]^{-1/2} \frac{\hbar^2}{2m_3} \mathbf{q}\cdot\mathbf{q}_1 S_3(q_1), \tag{7}$$

where $S(q_1)$ and $S_3(q_1)$ are the ^{4}He and impurity static structure functions.

In general, ME's involving $n-1$ phonon states, are expressed in terms of the n-body structure functions

$$S^{(n)}(\mathbf{q}_1, \ldots, \mathbf{q}_n) = \frac{1}{N_4} \frac{\langle\Psi_0|\rho_4^\dagger(\mathbf{q}_1)\cdots\rho_4^\dagger(\mathbf{q}_{n-1})\rho_4(\mathbf{q}_n)|\Psi_0\rangle}{\langle\Psi_0|\Psi_0\rangle}, \tag{8}$$

and

$$S_3^{(n)}(\mathbf{q}_1, \ldots, \mathbf{q}_n) = \frac{\langle\Psi_0|\rho_4^\dagger(\mathbf{q}_1)\cdots\rho_4^\dagger(\mathbf{q}_{n-1})\rho_3(\mathbf{q}_n)|\Psi_0\rangle}{\langle\Psi_0|\Psi_0\rangle}, \tag{9}$$

with $\mathbf{q}_n = \mathbf{q}_1 + \cdots + \mathbf{q}_{n-1}$.

The diagonal ME's have a particularly simple form:

$$\langle\mathbf{q};\mathbf{q}_1\cdots\mathbf{q}_n|\mathbf{q};\mathbf{q}_1\cdots\mathbf{q}_n\rangle = N_4^n S(q_1)\cdots S(q_n), \tag{10}$$

and

$$\langle\mathbf{q};\mathbf{q}_1\cdots\mathbf{q}_n|H|\mathbf{q};\mathbf{q}_1\cdots\mathbf{q}_n\rangle = E_0^v + e_0(q) + \sum_{i=1,n} w_F(q_i) \tag{11}$$

where $E_0^v = \langle\Psi_0|H|\Psi_0\rangle/\langle\Psi_0|\Psi_0\rangle$ and $w_F(q_i) = \hbar^2 q_i^2/2m_4 S_4(q_i)$ is the Feynman ^{4}He excitation spectrum.[13]

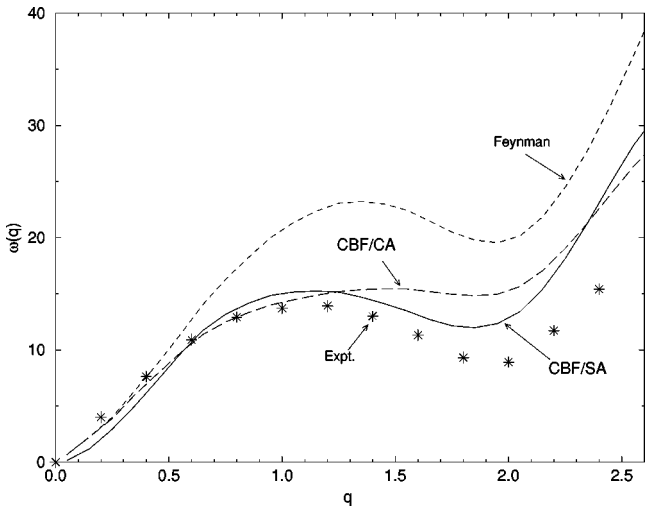

FIG. 1. ^{4}He excitation spectrum at equilibrium density. Stars are the experimental data. Energies in K and momenta in Å^{-1}.

The OIP and TIP perturbative diagrams contributing to $\Delta e(q)$ are shown in Fig. 5 of I, where only their $q=0$ derivative was computed, since the paper was concerned with just the calculation of the effective mass at $q=0$. Here we extend the formalism to finite q. We use Brillouin-Wigner perturbation theory, so the correction itself depends on $e(q)$ and the series must be summed self-consistently. For instance, the OIP contribution is given by

$$\begin{aligned}\Delta e_{\mathrm{OIP}}(q) &= \sum_{\mathbf{q}_1} \frac{|\langle\mathbf{q}|H - E_0 - e(q)|\mathbf{q};\mathbf{q}_1\rangle|^2}{e(q) - e_0(|\mathbf{q}-\mathbf{q}_1|) - w_F(q_1)} \\ &= \frac{\Omega}{(2\pi)^3}\left(\frac{\hbar^2}{2m_3}\right)^2 \int d^3q_1 \frac{1}{N_4 S(q_1)} \\ &\quad \times \frac{[S_3(q_1)\mathbf{q}\cdot\mathbf{q}_1]^2}{e(q) - e_0(|\mathbf{q}-\mathbf{q}_1|) - w_F(q_1)}.\end{aligned} \tag{12}$$

The expressions of the other diagrams are quite lengthy and will not be reported here. However, some comments are in order. They involve the two- and three-body structure functions, i.e., the Fourier transforms of the two- and three-body distribution functions $g^{(2)}(r_{12})$ and $g^{(3)}(\mathbf{r}_1,\mathbf{r}_2,\mathbf{r}_3)$. $g^{(2)}$ is a direct output of the HNC/Euler theory and, in pure ^{4}He, ends up very close to its experimental measurement. To evaluate $g^{(3)}$ is more involved and usually one has to resort to some approximations. The mostly common used are the convolution approximation (CA) and the Kirkwood superposition approximation (KSA).[10] The CA correctly accounts for the sequential relation between $g^{(3)}$ and $g^{(2)}$ and factorizes in momentum space, $S^{(3)}_{\mathrm{CA}}(\mathbf{q}_1,\mathbf{q}_2,\mathbf{q}_3) = S(q_1)S(q_2)S(q_3)$; the SA factorizes in r space, $g^{(3)}_{\mathrm{KSA}}(\mathbf{r}_1,\mathbf{r}_2,\mathbf{r}_3) = g^{(2)}(r_{12})g^{(2)}(r_{13})g^{(2)}(r_{23})$, and adequately describes the short-range region. The momentum space factorization property makes the use of the CA particularly suitable for our perturbative study.

The sensitivity of the calculation to the approximation for $g^{(3)}$ clearly shows up in the CBF-TIP evaluation of the ^{4}He excitation spectrum $\omega(q)$. Figure 1 compares the Feynman spectrum and those obtained within the CA and KSA with the experimental data. The phonon linear dispersion at low q

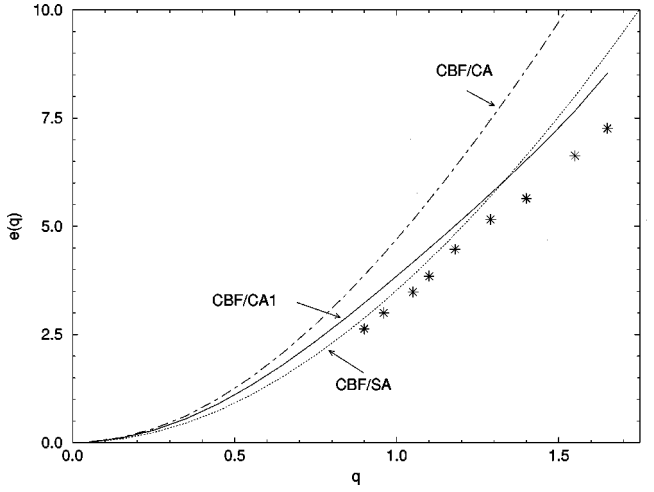

FIG. 2. ^{3}He single particle energies in CA, KSA, and CA1 without phonon rescattering. Stars are the experimental data. Units as in Fig. 1.

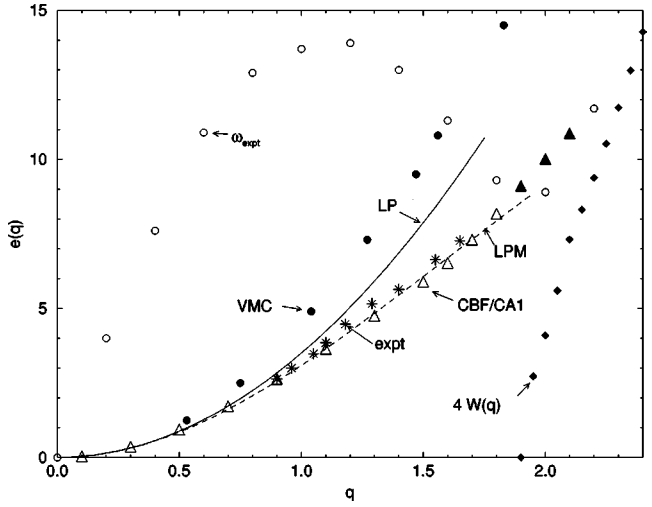

FIG. 3. CBF/CA1 (triangles), LP, and MLP ^{3}He single particle energies. Full circles are the VMC data. Stars and circles are the impurity and ^{4}He experimental data, respectively. Black triangles are extrapolated CBF/CA1 values (see text). Black diamonds give the impurity imaginary optical potential (in K). Units as in Fig. 1.

is well reproduced by both $\omega_F(q)$ and $\omega_{\rm CA}(q)$, whereas $\omega_{\rm KSA}(q)$ fails to give the correct behavior. As it is well known, the remaining part of the spectrum is severely overestimated by $\omega_F(q)$; both CA and KSA give a reasonable description of the maxon region but KSA is closer to the experiments at the roton minimum, because of its better description of the short-range regime. An overall good agreement with the experimental curve was obtained in Ref. 14 where backflow correlations were added to the CBF states.

Figure 2 shows $e(q)$ in CA and KSA, along with the data from Ref. 3. The curves do not include the ROP contribution. At this level, the effective masses are $m_3^*({\rm CA})=1.6m_3$ and $m_3^*({\rm KSA})=2.1m_3$ and again, KSA is closer to the experimental spectrum at large momenta. The curve labeled CA1 is obtained in CA, but using the experimental ^{4}He spectrum in the energy denominators. Diagram (5.e) of I, that gives the two-phonon correction to $\omega(q)$, has not been included as its effect is mostly taken into account by the use of $\omega_{\rm expt}(q)$. KSA and CA1 are close at large q values, pointing to a good description of the ^{4}He roton as a key ingredient for a correct approach to the large q sector. We will follow the CA1 method for the remainder of the work.

Figure 3 gives the CA1 impurity spectrum and the experimental ^{3}He and ^{4}He curves. The ROP terms are included and the LP and MLP fits to $e_{\rm expt}(q)$ are shown. Since the branch of the dynamical response due to the excitations of the low concentration ^{3}He component in the Helium mixtures overlaps the collective ^{4}He excitation at $q>1.7$ Å^{-1},[3,15] $e_{\rm expt}(q)$ is not known in that region. A rotonlike behavior was supposed in Ref. 9. This structure was not confirmed by the variational Monte Carlo (VMC) calculation of Ref. 8, which employed shadow wave functions in conjunction with a Jastrow correlation factor of the McMillan type. The VMC data at equilibrium density are given in the figure: they overestimate the experiment and have an effective mass of $m_3^*({\rm VMC})\sim 1.7m_3$.

The shadow wave function of Ref. 8 takes into account backflow effects. Actually, in several papers it was pointed out that second order perturbative expansion with OIP states introduces backflow correlations into the wave function.[5,16,17] We find $m_3^*({\rm OIP})=1.8m_3$, in good agreement with the VMC outcome. An analogous CBF treatment by Saarela[18] gave similar results ($m_3^*\sim 1.9m_3$) and a spectrum close to the LP form. More complicated momentum dependent correlations are generated by TIP and ROP diagrams, playing a relevant role in the CBF approach and giving $m_3^*({\rm CBF})=2.1m_3$.

The total CBF impurity spectrum is very close to $e_{\rm expt}(q)$ up to its merging into the ^{4}He dispersion relation. For the γ parameter in the MLP parametrization, the theory gives $\gamma({\rm CBF})\sim 0.19$ Å^2. If the spectrum is parametrized in terms of a momentum-dependent effective mass $e(q)=\hbar^2q^2/2m_3^*(q)$ then we find $m_3^*(q=1.7\ {\rm Å}^{-1})=3.2m_3$, with an increase of $\sim 50\%$ respect to the $q=0$ value.

Beyond $q\sim 1.9$ Å^{-1}, the energy denominators vanish for some momentum values and the series cannot be summed anymore. This is due to the fact that the impurity quasiparticle is no longer an excitation with a well defined energy, since it can decay into ^{4}He excitations and acquire a finite lifetime τ. A finite τ value reflects a nonzero imaginary part of the ^{3}He complex optical potential (or the on-shell self-energy) $W(q)={\rm Im}\,\Sigma[q,e(q)]$.[19] Figure 3 shows $W(q)$ as computed with only OIP intermediate states,

$$W_{\rm OIP}(q)=\pi\sum_{\mathbf{q}_1}|\langle\mathbf{q}|H-E_0-e(q)|\mathbf{q};\mathbf{q}_1\rangle|^2 \times\delta[e(q)-e_0(|\mathbf{q}-\mathbf{q}_1|)-w(q_1)], \qquad (13)$$

where the MLP impurity spectrum and the experimental ^{4}He dispersion have been used [notice that $W(q)$ is amplified by a factor 4 in the figure]. The OIP optical potential is close to the one found in Ref. 18. A numerical extrapolation of the computed $e_{\rm CBF}(q)$ into the roton region does not show any evidence of a ^{3}He rotonlike structure.

In conclusion, we find that CBF perturbative theory is able to give a quantitative description of the ^{3}He impurity

excitation spectrum in liquid ^{4}He at equilibrium density. The intermediate correlated states must consider at least two independent phonon states and one phonon state rescattering is found to play a nonmarginal role at large momenta. It is plausible that in a richer basis, including, for instance, explicit backflow correlations, a lower order expansion might be sufficient. However, the more complicated structure of the matrix elements could cause additional uncertainties in their evaluation, at least in the framework of the cluster expansion approach. The development of a Monte Carlo based algorithm for the computation of nondiagonal matrix elements would probably be the correct answer.

A.F. wants to thank the Institute for Nuclear Theory at the University of Washington for its hospitality and the Department of Energy for its partial support during the completion of this work. This research was also partially supported by DGICYT (Spain) Grant No. PB95-1249, the agreement CICYT (Spain)–INFN (Italy) and the Acción Integrada program (Spain-Italy).

[1] C. Ebner and D. O. Edwards, Phys. Rep., Phys. Lett. **2C**, 77 (1971).
[2] P. A. Hilton, R. Scherm, and W. G. Stirling, J. Low Temp. Phys. **27**, 851 (1978).
[3] B. Fåk, K. Guckelsberger, M. Korfer, R. Scherm, and A. J. Dianoux, Phys. Rev. B **41**, 8732 (1990).
[4] L. D. Landau and I. M. Khalatnikov, Zh. Eksp. Teor. Fiz. **19**, 637 (1948).
[5] A. Fabrocini, S. Fantoni, S. Rosati, and A. Polls, Phys. Rev. B **33**, 6057 (1986).
[6] M. Boninsegni and D. M. Ceperley, Phys. Rev. Lett. **74**, 2288 (1995).
[7] R. N. Bhatt, Phys. Rev. B **18**, 2108 (1978).
[8] D. E. Galli, G. L. Masserini, S. A. Vitiello, and L. Reatto, Czech. J. Phys. **46**, 295 (1996).
[9] L. P. Pitaevskii (unpublished).
[10] E. Feenberg, *Theory of Quantum Fluids* (Academic, New York, 1969).
[11] Q. N. Usmani, S. Fantoni, and V. R. Pandharipande, Phys. Rev. B **26**, 6123 (1982).
[12] R. A. Aziz, F. R. W. McCourt, and C. C. K. Wong, Mol. Phys. **61**, 1487 (1987).
[13] R. P. Feynman, Phys. Rev. **94**, 262 (1954).
[14] E. Manousakis and V. R. Pandharipande, Phys. Rev. B **33**, 150 (1986).
[15] A. Fabrocini, L. Vichi, F. Mazzanti, and A. Polls, Phys. Rev. B **54**, 10 035 (1996).
[16] T. B. Davison and E. Feenberg, Phys. Rev. **178**, 306 (1969).
[17] W. L. McMillan, Phys. Rev. **182**, 299 (1969).
[18] M. Saarela, *Recent Progress in Many Body Theories*, edited by Y. Avishai (Plenum, New York, 1990), Vol. 3, p. 337.
[19] S. Fantoni, B. L. Friman, and V. R. Pandharipande, Nucl. Phys. A **399**, 51 (1983).